Online Data Supplement

Thyroid hormone is highly permissive in angioproliferative pulmonary hypertension in rats

Aysar Al Husseini MD[1], Gianluca Bagnato MD[1], Laszlo Farkas MD[1], Jose Gomez-Arroyo MD[1], Daniela Farkas BSc[1], Shiro Mizuno MD PhD[1], Donatas Kraskauskas DVM[1], Antonio Abbate MD PhD[2], Benjamin Van Tassel Pharm D[2], Norbert F Voelkel MD[1] and Harm Jan Bogaard MD PhD[3]

Materials and Methods

Animal models

All rats received a normal diet (7012 Teklad LM-485 Mouse/Rat Sterilizable Diet, Harlan Laboratories, Inc.). Before tissue harvests, echocardiographic measurements were made of the RV internal diameter. RV pressure was assessed with a Millar catheter; PVR and cardiac output were determined by invasive hemodynamic measurements. Each rat was anesthetized with an intramuscular injection of ketamine/xylazine. The thoracic cavities were opened by midline incision, and a small sample of blood was obtained by cardiac puncture and placed in a heparinized tube for plasma T4 level determination. The right lung was removed, and frozen in liquid nitrogen. The left lung was inflated with 0.5% low-melting agarose at a constant pressure of 25cm H_2O, fixed in 10% formalin for 48 hours and used for small pulmonary arteries count and IHC analysis.

Assessment of angioproliferative vascular lesions

A quantitative analysis of luminal obstruction was performed by counting at least 200 small pulmonary arteries (OD, <50 um) per lung section from each rat in the 2 groups by two investigators blinded to the treatment group. Vessels were assessed for occlusive lesions on hematoxylin/eosin slides from two random left lung slices and scored as: no evidence of neointimal formation (patent); partially patent (<50%); and full-luminal occlusion (fully obliterated).

Antibodies

Rabbit anti-cleaved caspase-3 antibody, rabbit anti-PCNA antibody, rabbit anti- integrin αv antibody and rabbit anti-integrin β3 antibody (Cell Signaling Technology, Inc., Beverly, MA), mouse anti-phospho-Erk antibody, rabbit anti-Erk antibody, rabbit anti-phospho-AKT1/2/3 antibody, mouse anti-AKT1/2/3 antibody, rabbit anti-FGF2 antibody (Santa Cruz Biotechnology, Inc., Santa Cruz, CA), mouse anti-FGFR1 antibody, mouse anti- vWF (LifeSpan Biosciences, Inc., Seattle, WA),

rabbit anti- integrin αv (Abcam, Cambridge, MA), rabbit anti- vWF (Dako, Carpinteria, CA) and mouse anti-ß-actin antibody (Sigma, St. Louis, MO).

Western blot analysis

Whole cell lysate from one bole of the right lung was prepared using RIPA (Radio-Immunoprecipitation Assay) buffer (Sigma, St. Louis, MO), and the protein concentration was determined using BioRad Protein DC Protein Assay (BioRad, Hercules, CA). 15 µg of whole cellular protein per lane was separated by SDS-PAGE with a 4-12% Bis-Tris Nupage gel (MES SDS running buffer) and blotted onto a PVDF membrane. The membrane was incubated with blocking buffer (5% nonfat dry milk/PBS 0.1% Tween 20) at room temperature for 1 hour. The membrane was then probed with the primary antibodies diluted in blocking buffer overnight at 4˚C. Subsequently, membranes were incubated with horseradish peroxidase-conjugated anti-mouse or anti-rabbit antibody diluted 1:1000 in blocking buffer. Blots were developed with ECL (PerkinElmer, Waltham, MA) on GeneMate Blue Basic Autorad Films (BioExpress, Kaysville, UT). Each assay was performed in 6 independent experiments. Blots were scanned and densitometry analysis was done with ImageJ (National Institutes of Health 1997-2011, Bethesda, MD; http://imagej.nih.gov/ij).

Immunohistochemistry

IHC staining for cleaved caspase 3 and PCNA as well as the double immunofluorescence stainings for integrin αv/vWF, FGF2/vWF, FGFR1/vWF and pErk were performed according to standard protocols as previously published The following antibody dilutions were used: cleaved caspase3 1:200, PCNA 1:500, integrin αv 1:200, FGF2 1:10, FGFR1 1:50, pErk 1:5, rabbit anti- vWF 1:500, mouse anti- vWF 1:25. Images for cleaved caspase3 and PCNA were taken with AxioImager AX10, Axiocam MRm and Axiovision 3.1 software (Carl Zeiss, Göttingen, Germany). Optical sections were acquired by laser- scanning confocal microscopy with a Leica TCS-SP2 confocal microscope and images were analyzed and arranged with ImageJ. Microscopy was performed at the VCU Department of Anatomy and Neurobiology Microscopy Facility, supported, in part, with funding from NIH-NINDS Center core grant (5P30NS047463-02).

Statistical analysis

Differences between groups were assessed with analysis of variance (parametric) and Kruskall-Wallis (nonparametric) tests; Bonferroni (parametric) and Dunn (nonparametric) post hoc tests were used to assess for significant differences between pairs of groups. P values less than 0.05 were considered significant. For reasons of clarity, all data are reported as means ± SEM, unless specified otherwise, even if the differences between groups were tested with a nonparametric test that makes no use of means and standard deviations. Six to eight rats were used per group, unless specified otherwise.

Table 1 *Association between hyperthyroidism and pulmonary hypertension (PH) in clinical trials and case reports.*

Number of patients	*Diagnosis*	*Hyperthyroidism diagnosis before PAH diagnosis*	*sPAP before hyperthyroidism treatment (mmHg*	*sPAP after hyperthyroidism treatment (mmHg)*	*Improvement after treatment*	*Authors*
114 (43% with PH)	47=Graves; 67=MNG	yes	27±6	<25 (4 weeks)	yes	Marvisi (1)
75 (46% with PH)	30=Graves; 35=MNG	yes	48±1.2	34 ± 2 (24 weeks)	yes	Siu (2)
47 (34% with PH)	hyperthyroidism (unspecified)	yes	26±12	23 ± 10 (12 weeks)	yes	Guntekin (3)
33 (41% with PH)	hyperthyroidism (unspecified)	yes	36±12	29 ± 8 (56±32 weeks)	yes	Mercè (4)
23 (65% with PH)	22=Graves; 1=MNG	yes	36±8	26±5 (36 weeks)	yes	Armigliato (5)
25 (44% with PH)	7=Graves; 18=MNG	yes	30±8	24±5 (24 weeks)	yes	Yazar (6)
34 (group 1=not on therapy n=17; group 2=on therapy in euthyroid status n=17)	20=Graves; 14=MNG	yes (group 1)	28 ± 6 (group 1)	22±1 (group 2) (24±12 weeks)	yes	Marvisi (7)
1	Graves	yes (10 years)	35	21 (24 weeks)	yes	Thurnheer (8)
1	Graves	yes (20 years)	60	<25 (7 weeks)	yes	Wasseem (9)
1	MNG	yes (3 years)	65	45 (4 weeks)	yes	Mozo Herrera (10)
1	Graves	yes	68	30	yes	Nduwayo (11)
Total 353	128=Graves; 135=MNG; 80=hyperthyroidism (unspecified)	yes	41	27	yes	

sPAP = systolic pulmonary artery pressure estimated by echocardiography; MNG= multinodular goiter;

Table 2 *Genomic and non/genomic mechanisms of action of thyroid hormones.*

	Nuclear receptor pathway	*Membrane receptor pathway*	*Cytoplasmic pathway*
Cell growth	T3 - TRβ - cyclin D1 - cyclin dependent kinase - retinoblastoma protein - E2F pathway (12)	T4 - αvβ3 integrin - ERK 1/2 - STAT3 - EGF, FGF-2, VEGF (13)	
Cell proliferation		T4 - αvβ3 integrin -ERK 1/2 - STAT3 – EGF (14)	
Cell survival	T3 - TRβ1 - p53 inhibition(15)	T4 - αvβ3 integrin - MAPK - p53 inhibition (16)	T3 - interation between p85 subunit of PI3K and TRβ1 - AKT – HIF1α (17)
Angiogenesis		T4 - αvβ3 integrin - FGF-2, VEGF (18)	
Cell motility	T3 -TRβ binding to gelsolin (19)		
Cell migration		T4 – integrin/laminin interactions (20)	

STAT = Signal Transducer and Activator of Transcription; EGF = Epidermal Growth Factor; FGF = Fibroblast Growth Factor; VEGF = Vascular Endothelial Growth Factor; TR = Thyroid hormones Receptor; MAPK = Mitogen Activated Protein Kinases

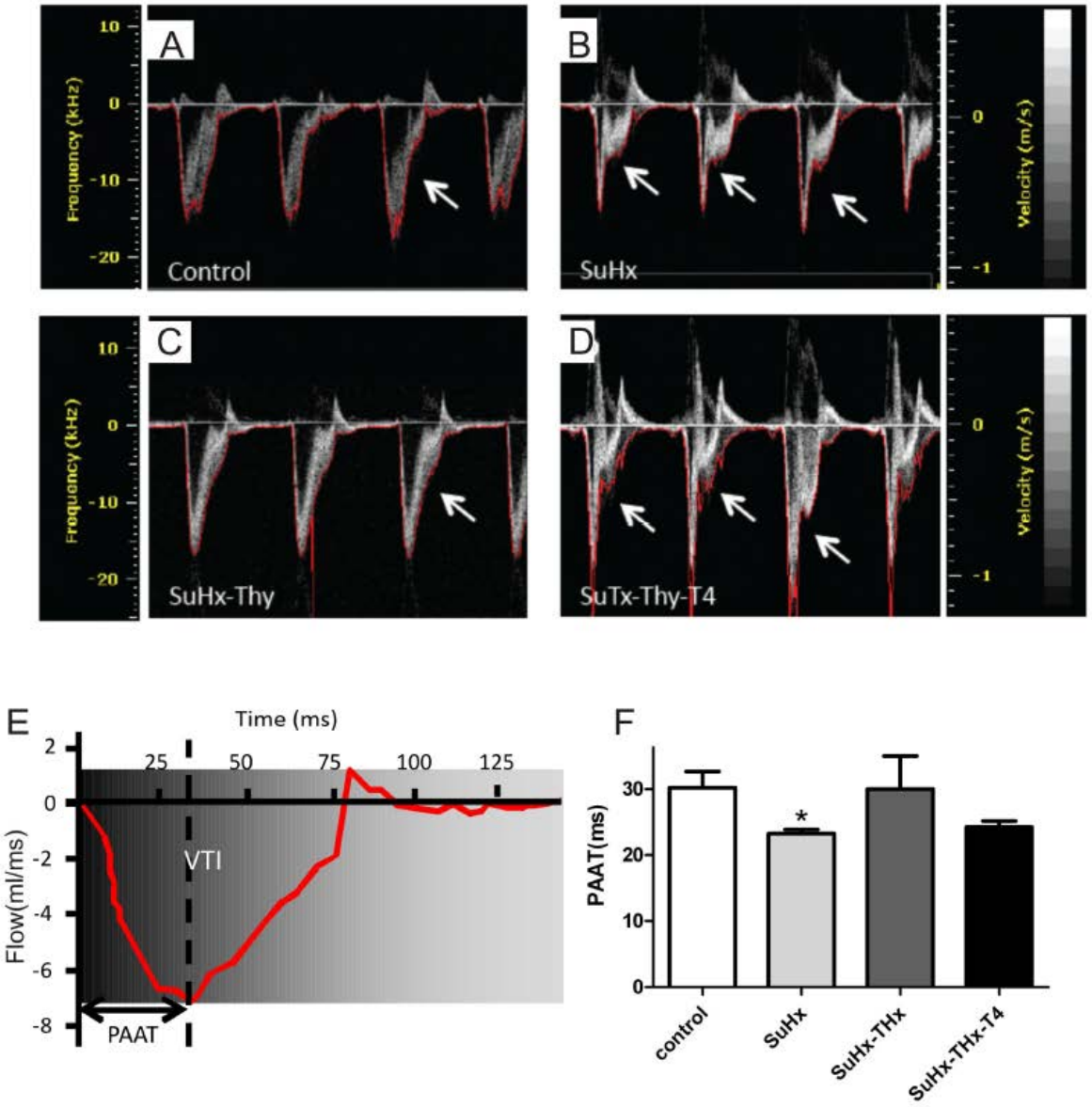

Supplemental Figure 1: (A-D) show representative images of pulmonary artery blood flow measurement use for the determination of velocity time integral (VTI) and pulmonary artery acceleration time (PAAT). (A) Shows the control rat. (B) Shows the SuHx rat with shortened PAAT. (C) Shows the SuHx rat with thyroidectomy and recovered PAAT. (D) Shows the SuHx rat with thyroidectomy plus T4 supplementation in which the PAAT is also reduced. (E) Illustrates the processes for VTI and PAAT measurements. (F) Displays the quantified PAAT measurements by each treatment group and indicates a significant reduction in PAAT in SuHx rat in comparison to Control rat.

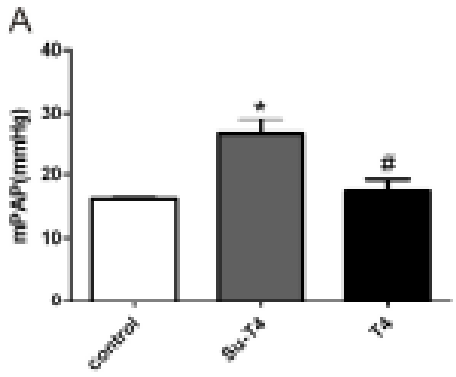

Supplemental Figure 2: (A) Shows the mean pulmonary artery pressure of control rats, Sugen (SU5416) only plus T4 rats and T4 only rats. Data expressed as mean ± SE (n=6).

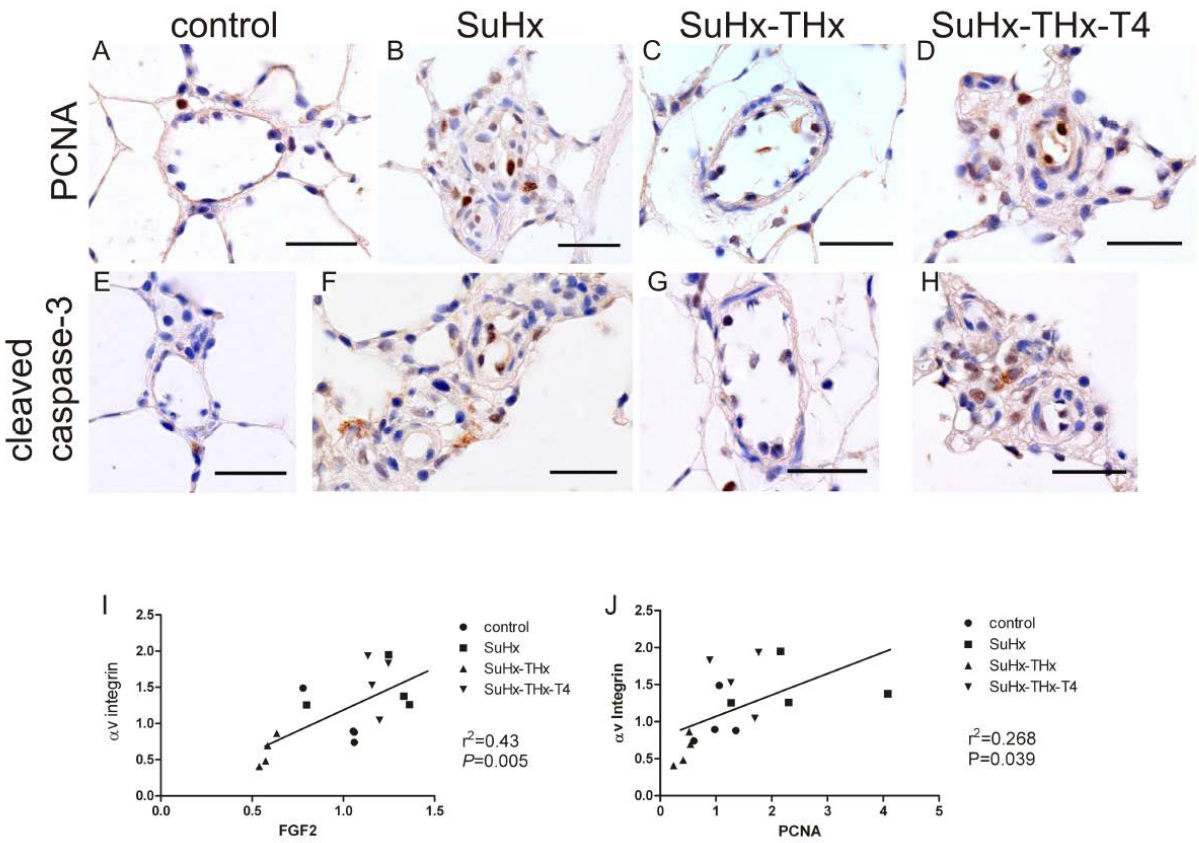

Supplemental Figure 3: (A-D) Show representative photomicrograph of PCNA stained lung sections of control rat (A), SuHx rat (B), SuHx rat with thyroidectomy (C) and SuHx rat with thyroidectomy with T4 replacement (D). (E-H) Show representative photomicrograph of cleaved caspase-3 stained lung sections of control rat (E), SuHx rat (F), SuHx rat with thyroidectomy (G) and SuHx rat with thyroidectomy with T4 replacement (H). (A-H) are 40X magnification, scale bar 30µm. αv integrin is correlated with FGF2 (I) and with PCNA (J) protein expression from the whole lung tissue.

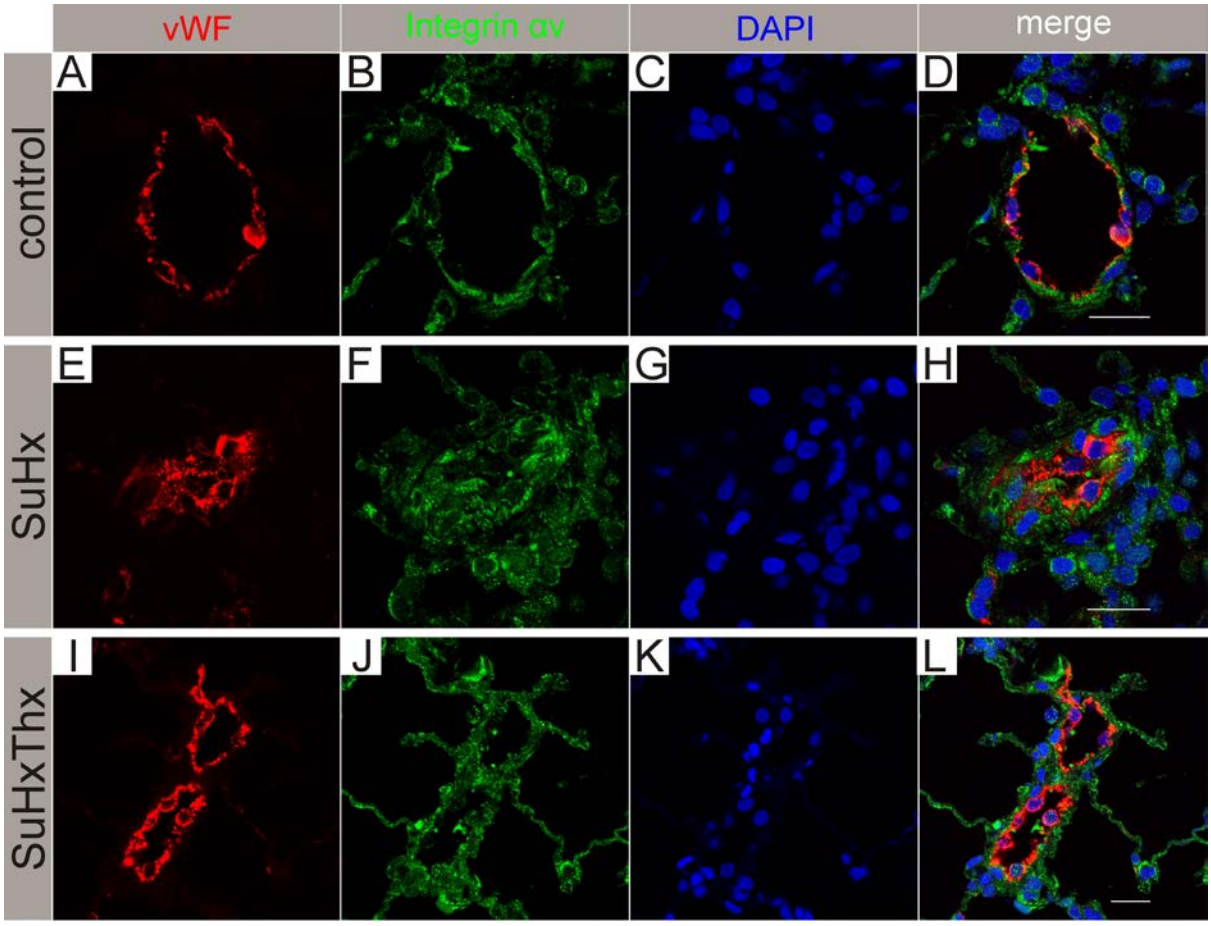

Supplemental Figure 4: Representative optical sections acquired by confocal microscopy of double immunofluorescence stainings for vWF/integrin αv. **(A-D)** shows the single channels and merged image for control animal from **Figure 4A. (E-H)** shows the single channels and merged image for SuHx treated animal from **Figure 6B. (I-L)** shows the single channels and merged image for SuHxThx treated animal from **Figure 6C.** vWF+ (red) endothelial cells are shown in **A, E, I**. Integrin αv+ staining in the green channel is demonstrated in **B, F, J**. Nuclear counterstaining with DAPI (blue) is shown in **C, G, K**. The merged image from all three channels is found in **D, H, L**. Scale bar is 20µm.

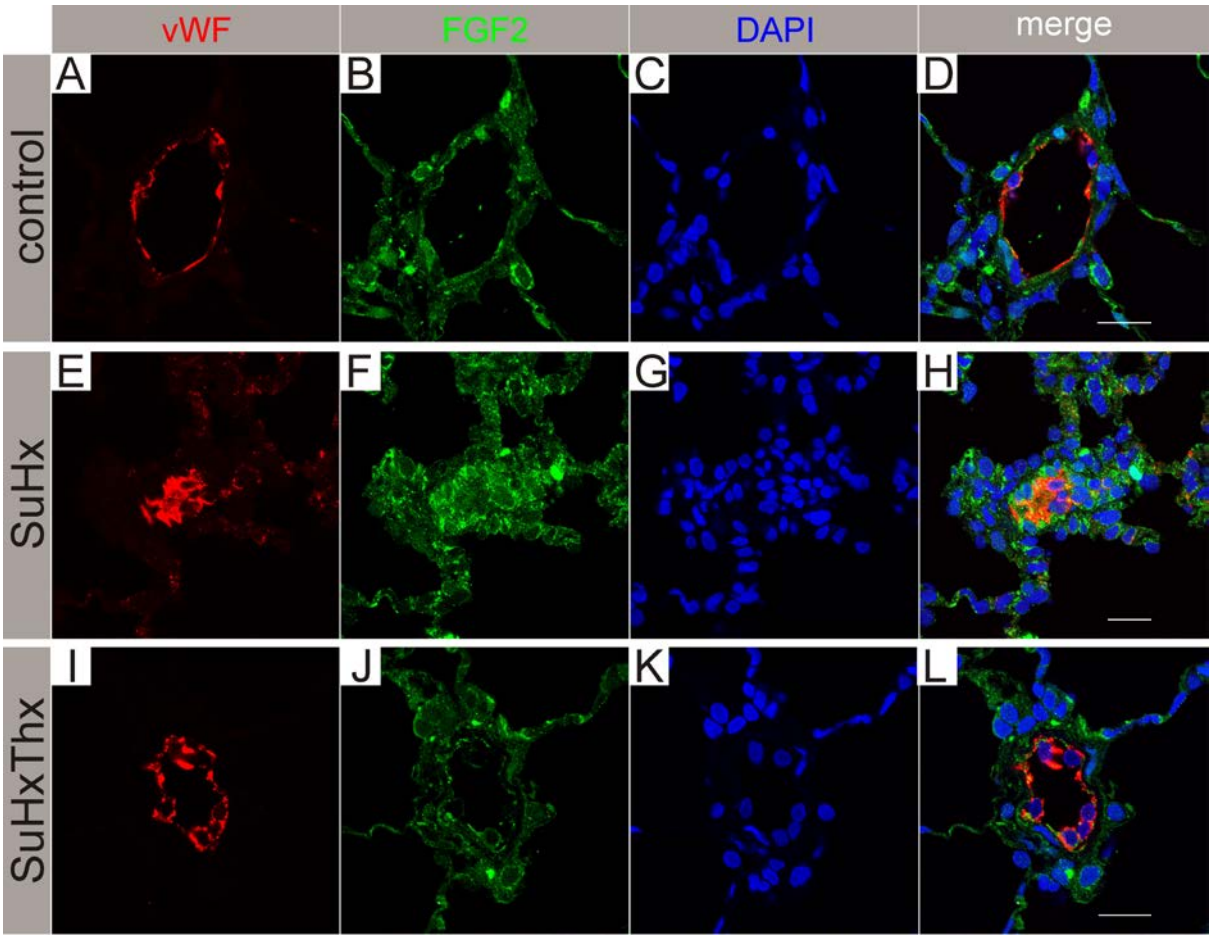

Supplemental Figure 5: Representative optical sections acquired by confocal microscopy of double immunofluorescence stainings for vWF/FGF2. **(A-D)** shows the single channels and merged image for control animal from **Figure 6D. (E-H)** shows the single channels and merged image for SuHx treated animal from **Figure 6E. (I-L)** shows the single channels and merged image for SuHxThx treated animal from **Figure 6F.** vWF+ (red) endothelial cells are shown in **A, E, I**. FGF2+ staining in the green channel is demonstrated in **B, F, J**. Nuclear counterstaining with DAPI (blue) is shown in **C, G, K**. The merged image from all three channels is found in **D, H, L**. Scale bar is 20µm.

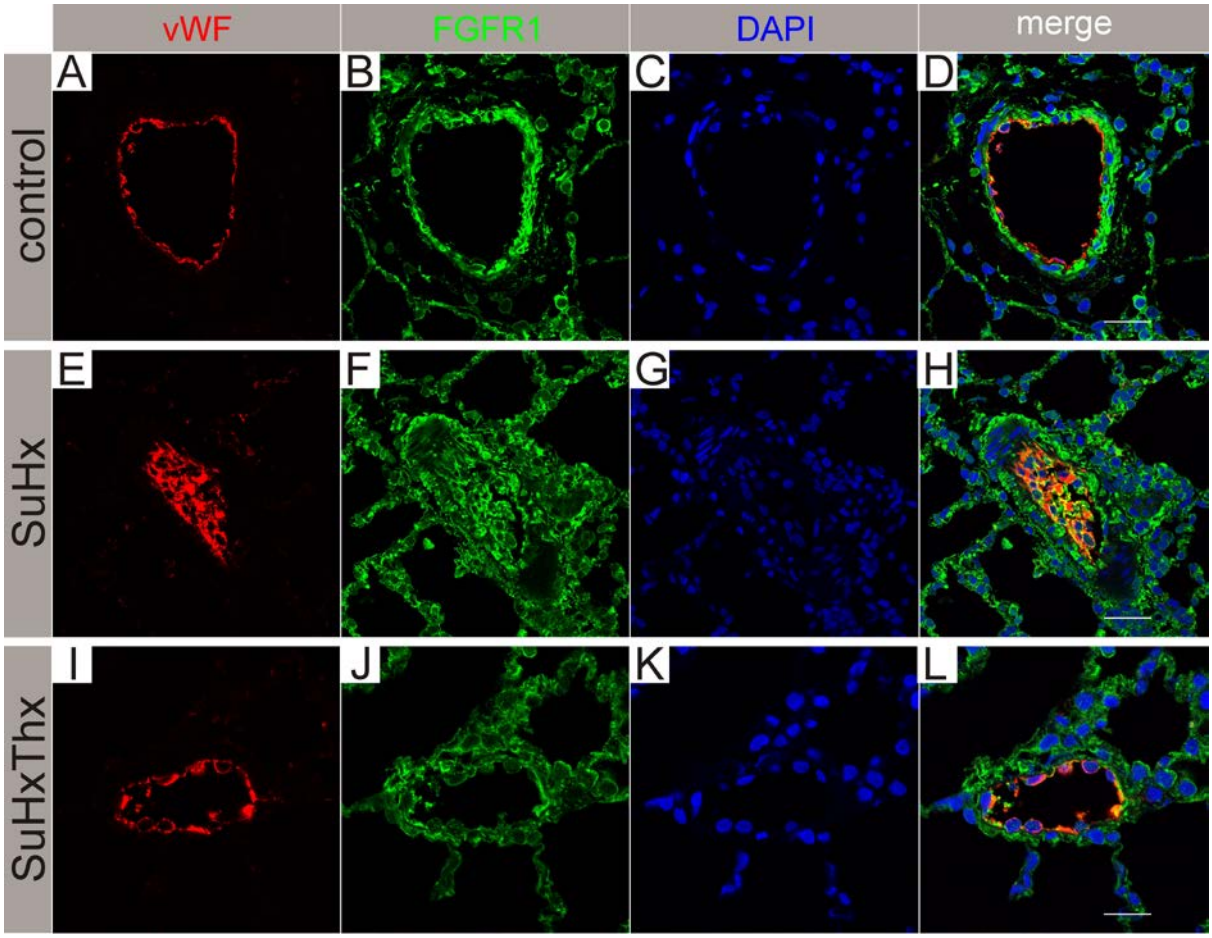

Supplemental Figure 6: Representative optical sections acquired by confocal microscopy of double immunofluorescence stainings for vWF/FGFR1. **(A-D)** shows the single channels and merged image for control animal from **Figure 6G. (E-H)** shows the single channels and merged image for SuHx treated animal from **Figure 6H. (I-L)** shows the single channels and merged image for SuHxThx treated animal from **Figure 6I.** vWF+ (red) endothelial cells are shown in **A, E, I**. FGFR1+ staining in the green channel is demonstrated in **B, F, J**. Nuclear counterstaining with DAPI (blue) is shown in **C, G, K**. The merged image from all three channels is found in **D, H, L**. Scale bar is 20µm.

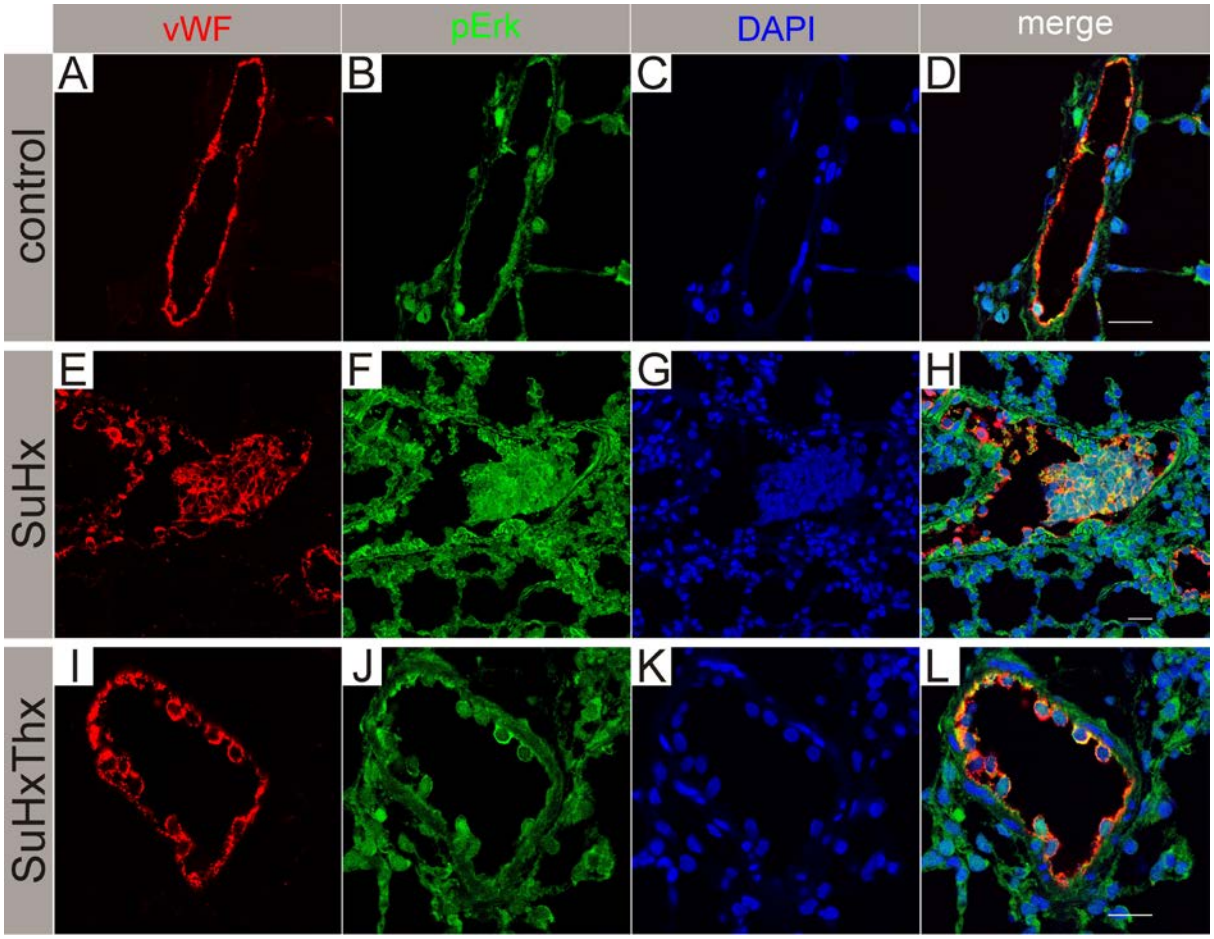

Supplemental Figure 7: Representative optical sections acquired by confocal microscopy of double immunofluorescence stainings for vWF/pErk1/2. **(A-D)** shows the single channels and merged image for control animal from **Figure 6J. (E-H)** shows the single channels and merged image for SuHx treated animal from **Figure 6K. (I-L)** shows the single channels and merged image for SuHxThx treated animal from **Figure 6L.** vWF+ (red) endothelial cells are shown in **A, E, I**. pErk1/2+ staining (in the nucleus and cytoplasm) in the green channel is demonstrated in **B, F, J**. Nuclear counterstaining with DAPI (blue) is shown in **C, G, K**. The merged image from all three channels is found in **D, H, L**. Scale bar is 20µm.

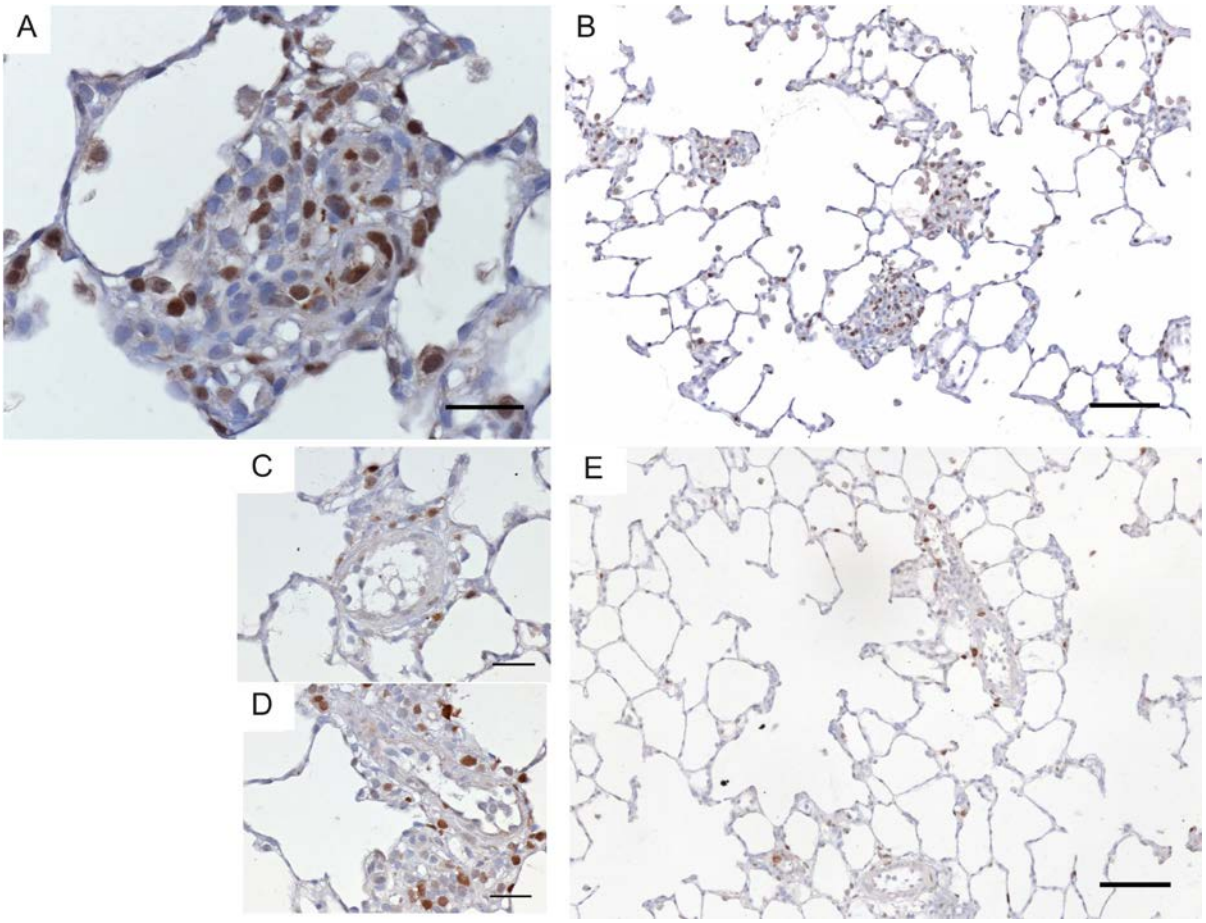

Supplemental Figure 8: (A-D) Show representative photomicrograph of PCNA stained lung sections of SuHx rat (A, B), SuHx rat treated with PTU (C, D, E). (A, C, D) are 40Xmagnification, scale bar is 30µm and (B, E) are 10X magnification, scale bar is 100µm.

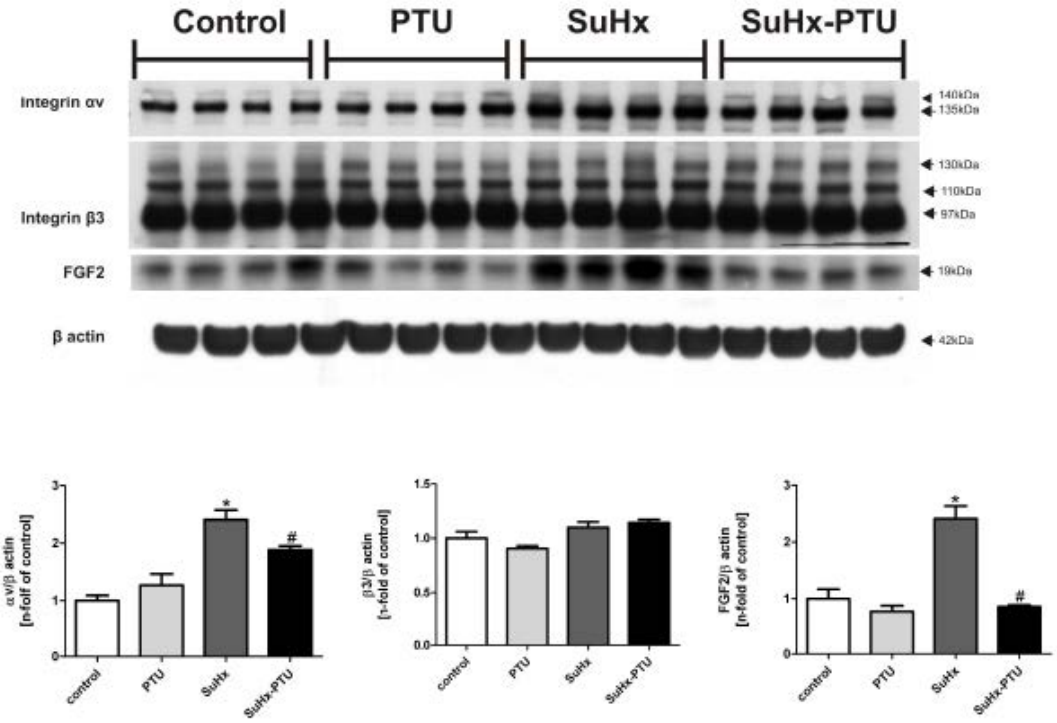

Supplemental Figure 9: (A) Representative western blot analysis of Integrin αv, Integrin β3, FGF2 and β-actin in lung protein extracts from control, SuHx, SuHx rats treated with PTU. (B-D) The bar graphs show the ratios of Integrin αv, Integrin β3 and FGF2 ratio protein expression relative to controls. Data are expressed as mean ± SE (n=4). *P <0.05 versus control and #P <0.05 versus SuHx.

Reference List

(1) Marvisi M, Zambrelli P, Brianti M, Civardi G, Lampugnani R, Delsignore R. Pulmonary hypertension is frequent in hyperthyroidism and normalizes after therapy. Eur J Intern Med 2006 July;17(4):267-71.

(2) Siu CW, Zhang XH, Yung C, Kung AW, Lau CP, Tse HF. Hemodynamic changes in hyperthyroidism-related pulmonary hypertension: a prospective echocardiographic study. J Clin Endocrinol Metab 2007 May;92(5):1736-42.

(3) Guntekin U, Gunes Y, Tuncer M, Simsek H, Gumrukcuoglu HA, Arslan S, Gunes A. QTc dispersion in hyperthyroidism and its association with pulmonary hypertension. Pacing Clin Electrophysiol 2009 April;32(4):494-9.

(4) Merce J, Ferras S, Oltra C, Sanz E, Vendrell J, Simon I, Camprubi M, Bardaji A, Ridao C. Cardiovascular abnormalities in hyperthyroidism: a prospective Doppler echocardiographic study. Am J Med 2005 February;118(2):126-31.

(5) Armigliato M, Paolini R, Aggio S, Zamboni S, Galasso MP, Zonzin P, Cella G. Hyperthyroidism as a cause of pulmonary arterial hypertension: a prospective study. Angiology 2006 October;57(5):600-6.

(6) Yazar A, Doven O, Atis S, Gen R, Pata C, Yazar EE, Kanik A. Systolic pulmonary artery pressure and serum uric acid levels in patients with hyperthyroidism. Arch Med Res 2003 January;34(1):35-40.

(7) Marvisi M, Brianti M, Marani G, Del BR, Bortesi ML, Guariglia A. Hyperthyroidism and pulmonary hypertension. Respir Med 2002 April;96(4):215-20.

(8) Thurnheer R, Jenni R, Russi EW, Greminger P, Speich R. Hyperthyroidism and pulmonary hypertension. J Intern Med 1997 August;242(2):185-8.

(9) Wasseem R, Mazen E, Walid SR. Hyperthyroidism: a rare cause of reversible pulmonary hypertension. Am J Med Sci 2006 September;332(3):140-1.

(10) Mozo HG, Fernandez Gonzalez MJ, Salgado BJ, Jimeno CA. [Hyperthyroidism, jaundice, and pulmonary hypertension]. An Med Interna 2001 May;18(5):262-4.

(11) Nduwayo L, Pop C, Heim J. [Reversible pulmonary hypertension in Basedow's disease]. Presse Med 2000 December 23;29(40):2216-8.

(12) Furumoto H, Ying H, Chandramouli GV, Zhao L, Walker RL, Meltzer PS, Willingham MC, Cheng SY. An unliganded thyroid hormone beta receptor activates the cyclin D1/cyclin-dependent kinase/retinoblastoma/E2F pathway and induces pituitary tumorigenesis. Mol Cell Biol 2005 January;25(1):124-35.

(13) Davis PJ, Davis FB, Mousa SA, Luidens MK, Lin HY. Membrane receptor for thyroid hormone: physiologic and pharmacologic implications. Annu Rev Pharmacol Toxicol 2011 February 10;51:99-115.

(14) Lin HY, Shih A, Davis FB, Davis PJ. Thyroid hormone promotes the phosphorylation of STAT3 and potentiates the action of epidermal growth factor in cultured cells. Biochem J 1999 March 1;338 (Pt 2):427-32.

(15) Barrera-Hernandez G, Zhan Q, Wong R, Cheng SY. Thyroid hormone receptor is a negative regulator in p53-mediated signaling pathways. DNA Cell Biol 1998 September;17(9):743-50.

(16) Lin HY, Tang HY, Shih A, Keating T, Cao G, Davis PJ, Davis FB. Thyroid hormone is a MAPK-dependent growth factor for thyroid cancer cells and is anti-apoptotic. Steroids 2007 February;72(2):180-7.

(17) Lin HY, Sun M, Tang HY, Lin C, Luidens MK, Mousa SA, Incerpi S, Drusano GL, Davis FB, Davis PJ. L-Thyroxine vs. 3,5,3'-triiodo-L-thyronine and cell proliferation: activation of mitogen-activated protein kinase and phosphatidylinositol 3-kinase. Am J Physiol Cell Physiol 2009 May;296(5):C980-C991.

(18) Tomanek RJ, Zimmerman MB, Suvarna PR, Morkin E, Pennock GD, Goldman S. A thyroid hormone analog stimulates angiogenesis in the post-infarcted rat heart. J Mol Cell Cardiol 1998 May;30(5):923-32.

(19) Kim CS, Furuya F, Ying H, Kato Y, Hanover JA, Cheng SY. Gelsolin: a novel thyroid hormone receptor-beta interacting protein that modulates tumor progression in a mouse model of follicular thyroid cancer. Endocrinology 2007 March;148(3):1306-12.

(20) Farwell AP, Dubord-Tomasetti SA, Pietrzykowski AZ, Stachelek SJ, Leonard JL. Regulation of cerebellar neuronal migration and neurite outgrowth by thyroxine and 3,3',5'-triiodothyronine. Brain Res Dev Brain Res 2005 January 1;154(1):121-35.